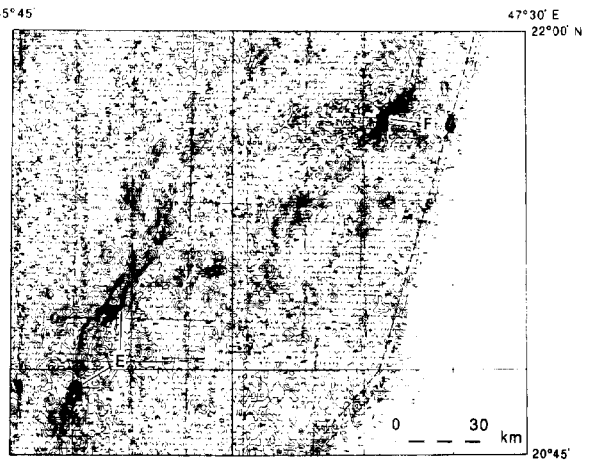

FIG. 6. eU contour map of an area of radiometric anomalies in Cretaceous rocks of southern Saudi Arabia. Contour interval 0.2 and 1.0 ppm eU. Flight line number, location, fiducial tick and number, e.g., 24 860, 4 000. Letters indicate locations discussed in text. Heavy dashed line is boundary of aerial survey.

Anomalies C and C′ are in the Cambro-Ordovician Wajid sandstone and are associated with ferruginous horizons in quartzarenite of the Ilman member. These horizons are iron-cemented sandstone, conglomeratic sandstone, siltstone, and mudstone beds, which are probably the sources of the anomalies of Figure 4, although not all anomalies were visited during this investigation. Anomalies seemingly coincident for all three radioelements also occur in Wajid rocks. These anomalies are labeled D on Figures 4 and 5 where eU (Figure 4) is 2.0 to >5.0 ppm in a background of 1.5 to 2.0 ppm, eTh (Figure 5) is 7 to >13 ppm in a background of 4 to 6 ppm, and K (not shown) is 0.5 to 1.5 percent K in a background of 0.1 to 0.5 percent. Ground investigations show that anomaly D, seemingly coincident for all radioelements measured by the airborne survey, actually results from near superposition of adjacent stratigraphic horizons in nearly horizontal strata, also in the Ilman member of the Wajid sandstone. The anomalous eTh appears to be from a horizon of thorium-bearing heavy minerals, the anomalous K is evidently from several horizons of potassic feldspar or potassic mica, and the anomalous eU is from several ferruginous horizons. Ground measurments in the area of D included local highs of about 10 ppm eU, 40 ppm eTh, and 1.0 to >2.0 percent K.

Anomalies in Cretaceous rocks are wholly eU (Figure 6). Anomaly E is in the outcrop of the Lower Cretaceous Biyadh sandstone and anomaly F is in the outcrop of the Middle Cretaceous Wasia formation. Anomaly E (Figure 6) is 2.0 to >4.0 ppm eU in a background of 1.4 to 2.0 ppm, and has a slight correspondence with eTh and K contours (neither shown). For the area of E, eTh is about 2 to 5 ppm eTh and K is about 0.3 to 0.8 percent K. Anomaly F (Figure 6) is 2.0 to >5.0 ppm eU in a background of 1.4 to 2.0 ppm. It has no expression in the eTh or K data (not shown). For the area of anomaly F, eTh is about 3 to 5 ppm and K is about 0.3 to 0.5 percent. Local ground highs were about 25 ppm eU in the area of anomaly E and about 30 ppm eU in the area of anomaly F. The eU anomalies are associated with ferruginous horizons in sandstone and conglomeratic sandstone, similar to the Wajid anomalies.

The presence of uraniferous ironstone in rocks of Paleozoic and Mesozoic age, as indicated by aerial and ground eU measurements, is a phenomenon not readily explained. A reasonable hypothesis is coeval mineralization by ground waters moving through the continental detrital rocks sometime after the latest Cretaceous. This hypothesis suggests the possibility of uranium mineralization downdip in the Phanerozoic section because of the availability of soluble and mobile uranium in the geologic past.

Work in progress

Sampling for radioactivity, mineralogic, and geochemical analyses was conducted in the areas of ground investigations. We are currently analyzing these data and extrapolating more detail of the characteristics and sources of the aerial radioactivity anomalies.

References

Matzko, J. J., Flanigan, V. J., Mawad, Mustafa, Al Kollak, Ziad, Naqvi, M. I., and Helaby, A. M., 1978, Radioactive anomaly and mineralogy of the lower part of the Tabuk Formation, Al Qassim area, Kingdom of Saudi Arabia: U.S. Geol. Surv. Saudi Arabia Project rep. 220, 22 p.

Merghelani, Habib, Kane, M. F., Cowan, D. R., and Pitkin, J. A., 1985, Regional aeromagnetic and aeroradiometric investigations of the cover-rock region, Saudi Arabia: Presented at the 55th Annual SEG Meeting, Washington, DC.

Pitkin, J. A., and Huffman, A. C., Jr., 1986, Geophysical and geological investigations of aerial radiometric anomalies in the Tabuk Formation of northwestern Saudi Arabia: A preliminary report: U.S. Geol. Surv. Saudi Arabian Mission Open-file rep. OF-05-10, 20 p.

———in press, Geophysical and geological investigations of aerial radiometric anomalies in the Phanerozoic cover rocks of southern Saudi Arabia: A preliminary report: U.S. Geol. Surv. Saudi Arabian Mission Open-file rep., 23 p.

Time-Domain Response of a Thin Plate Beneath Overburden — MIN 1.7

David C. Bartel and A. Becker, University of California, Berkeley

Numerical modeling of the time-domain response of a thin sheet target beneath a thin conductive overburden for the horizontal coaxial dipole configuration shows that the magnetic field response of the target must first build up, then decay. The time interval when the target response exceeds the overburden response defines a window of target detectability. A contrast of at least 5 between the target conductance and the conductance of the overburden is necessary for detection. This contrast may increase depending on many factors, including target depth, target size, and height-to-dipole separation (*h/l*) ratio. The overburden response is sensitive to the *h/l* ratio, and target detection capability is diminished as the *h/l* ratio is lessened. The resistivity of the host rock containing the target does not seem to have a large effect on target detection. The use of a finite length current pulse will affect the response, particularly at early times, and may lead to a deterioration in the ability to detect the target. Most electromagnetic (EM) exploration systems measure the voltage induced in the receiver coil, and thus relatively amplify the overburden response at early times. The window of target detectability can be predicted, allowing an explorationist to adjust his survey parameters accordingly.

Introduction

Time-domain EM exploration involves the measurement of transient magnetic fields after current turn-off in the transmitter. Our modeling study is for the magnetic field step response of a thin plate target in a two-layer earth. The EM system consists of two horizontal coaxial dipoles. While it is known that conductive overburden delays and attenuates the response of a conductive

target beneath it (Spies, 1980), the exact mechanism has not been studied well. Previous work in the frequency- and time-domains on the response of layered spheres shows that at high frequencies or at early times, the response is controlled by the outer layer, and that at low frequencies or at late times, the outer layer becomes invisible, and only the inner core response is detectable (Fuller, 1971; Nabighian, 1971). For a target beneath overburden, one would expect that only the overburden is visible at early times; and at late times, the target would be detectable. However, the overburden response will again dominate over the target response at some late time. This occurs because the target response decays exponentially with time, while the overburden response decays as an inverse power of time. This window of target detectability in the time-domain has been observed in field cases such as for the Elura orebody (Spies, 1980).

Modeling programs

Our approach to the problem is to assume a vertical thin sheet target beneath a conductive overburden. The magnetic field response to this model earth, using horizontal coaxial transmitter and receiver dipoles, was calculated using program SHEET. Originally, this program was developed only for frequency-domain calculations (Weidelt, 1981). It calculates separately the layered earth response (overburden + host) and the target response with proper consideration of its location under the overburden and in the host rock. Recently, use of the program was extended to the time-domain by augmenting the program with a fast Fourier transform subroutine. This allowed us to obtain the step response for the target. We found it simpler, however, to obtain the layered earth response by assuming an infinite, thin, overburden sheet and a very resistive host rock. The secondary magnetic field due to the overburden is given by (Grant and West, 1965, p. 498):

$$H_x^s(t) = \frac{-m[r_t^2 - 3l^2]}{4\pi r_t^5}, \tag{1}$$

where

$$r_t^2 = l^2 + 4\left[h + \frac{t}{\mu_0 \sigma s}\right]^2. \tag{2}$$

The height of the transmitting and receiving dipoles above the thin sheet is h, and the separation is l. The dipole strength of the transmitter is m, μ_0 is the magnetic permeability of free-space, and σs is the conductance of the thin sheet.

Model geometry

Figure 1 shows the system configuration and model parameters for this study. The standard target model is a vertical thin sheet of conductance $\sigma_2 s_2$, 300 m by 300 m, at some depth (D) beneath the surface. The overburden is a thin sheet of conductance $\sigma_1 s_1$, and the host rock resistivity is 10 000 $\Omega \cdot m$. The transmitter and receiver dipoles are maintained at .50 m above the overburden sheet. Profiles were run over the center of the target.

Modeling results

Normalization. The results of any modeling study, numerical or analog, can be most succinctly presented by making use of the EM scaling relationships (Spies, 1980). In our case, we chose the independent length variable to be the height of the coaxial dipole system above the overburden. All other distances (e.g., dipole separation) are normalized to this measure. We chose the conductance contrast between the target and overburden as the

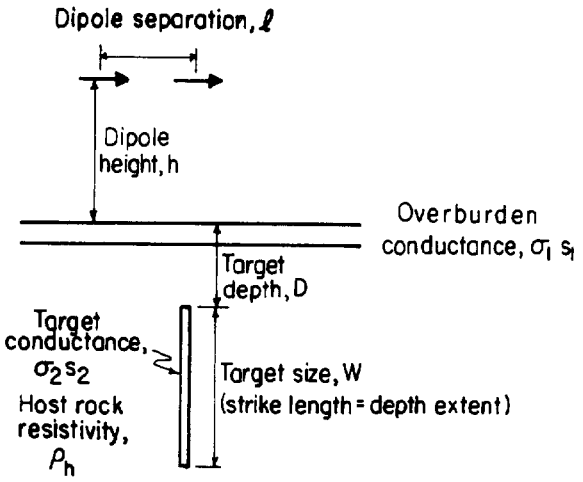

FIG. 1. Model geometry cross-section.

other free variable. With these choices, we can present the results as a function of normalized time using the overburden conductance for the normalization to get

$$\tau_1 = \frac{t}{\mu_0 \sigma_1 s_1 h}. \tag{3}$$

Alternatively, we can use the target conductance for the normalization to get

$$\tau_2 = \frac{t}{\mu_0 \sigma_2 s_2 h}. \tag{4}$$

Equation (3) is satisfactory for most purposes. If, however, we wish to study the effect of a variable overburden on the target responses, it is more convenient to normalize the time scale by the target conductance [equation (4)]. The amplitudes were nor-

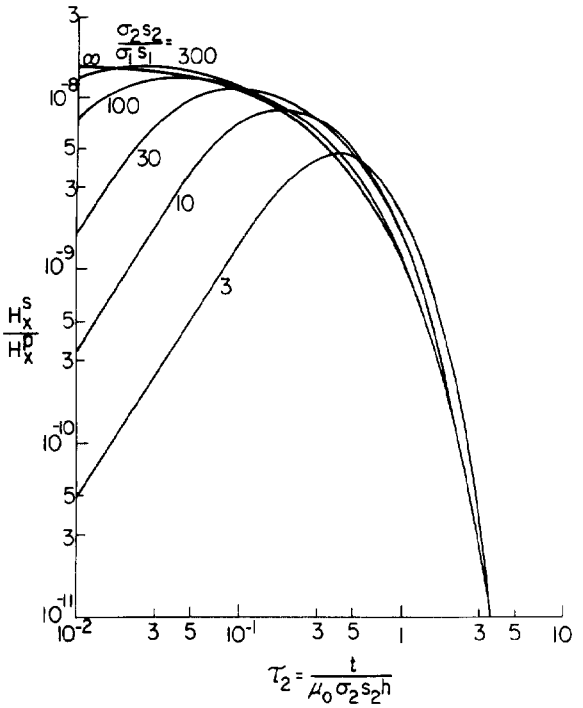

FIG. 2. SHEET versus free-space models; $h/l = 50$, $h = 50$ m, $D = 30$ m, $W = 300$ m, dipoles straddling target.

malized by the free-space primary magnetic field at the receiver dipole.

Influence of overburden on target response. It is known that the secondary magnetic field of a target in free space reaches its maximum value at the instant of primary field extinction. It then decreases from this initial value so that at some late time, the target response can be represented by an exponential decay (Kaufman, 1978). When, however, a conducting overburden exists between the transmitter and target, the extinction of the primary field at the target is delayed by eddy currents induced in the overburden. Consequently, the target response is also delayed. It first builds up slowly from zero to some maximum value, and then decays in a manner similar to its free-space response. The early-time magnetic field buildup is illustrated in Figure 2 for different $\sigma_2 s_2/\sigma_1 s_1$ contrasts. The magnetic field is smaller and takes longer to asymptote to the free-space ($\sigma_2 s_2/\sigma_1 s_1 = \infty$) value as the conductance contrast decreases. The early-stage (small τ_2) magnetic field increase appears to be proportional to $t^{3/2}$. High contrast models quickly asymptote to the free-space response. The target responses beneath an overburden slightly exceed those in free space at some τ_2 values because of galvanic enhancement.

Target detection. If we consider the target response as signal and the overburden response as noise, then for target detection, the signal-to-noise ratio (S/N) must at least equal unity. Thus the quantities of interest are τ_{early}, the value of τ_1 at which the S/N first reaches unity, and τ_{late} which denotes the time where the overburden response once again dominates. Figure 3 presents the numerical modeling results for $h/l = 50$ and $D = 30$ m, where the conductance contrast between the target and overburden is varied. From Figure 3, it can be seen that the target conductance must be at least 7 times larger than the overburden conductance if the target is to be detected. The S/N may also be considered a

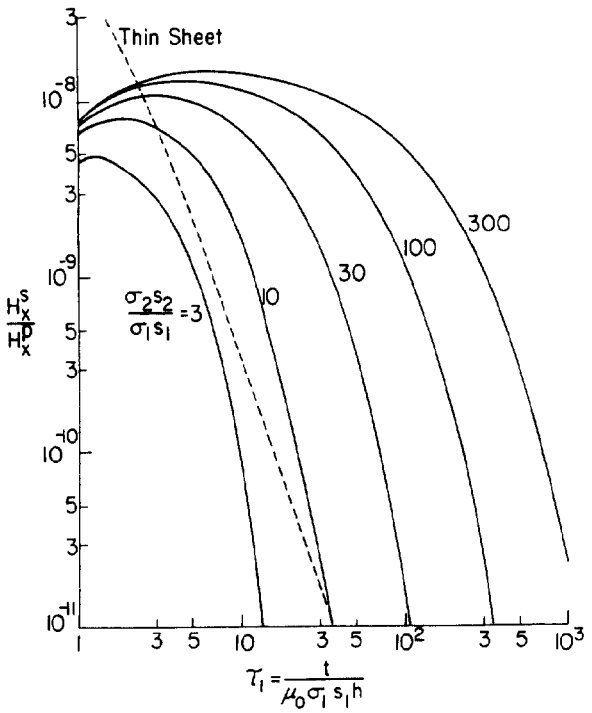

FIG. 3. Target and overburden responses for $h/l = 50$ and $D = 30$ m; $h = 50$ m, $W = 300$ m, dipoles straddling target.

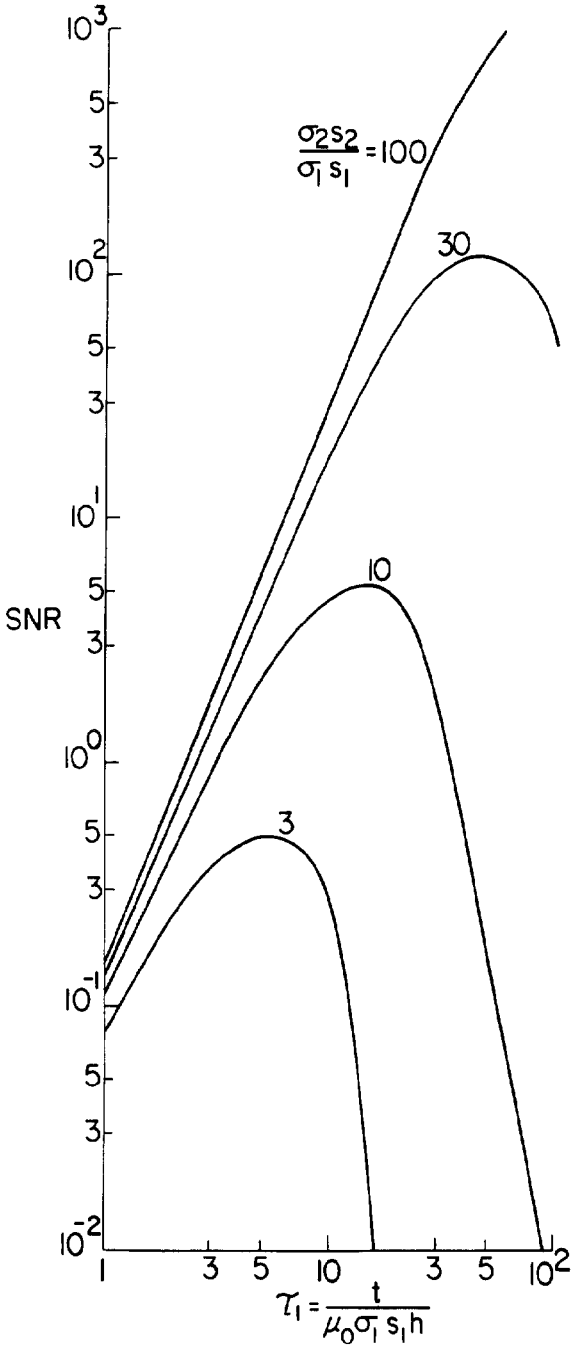

FIG. 4. S/N versus τ_1 for $h/l = 50$ and $D = 30$ m; curves are for various $\sigma_2 s_2/\sigma_1 s_1$ contrasts, $h = 50$ m, $W = 300$ m, dipoles straddling target.

function of time and conductivity contrast (Figure 4). The conductance contrast is the main influence on the maximum observable S/N. On the other hand, the S/N at low τ_1 values is largely independent of the target-overburden conductance ratio.

Effect of system geometry. Both the overburden and target responses change with the h/l ratio. In the limits, we may consider $h/l \approx \infty$ when the transmitting and receiving dipoles are essentially coincident, and $h/l \approx 0$ when the dipoles are far apart and/or on the surface. Changes in the h/l ratio mainly affect the overburden response. The ability to distinguish a conductive target beneath overburden also varies with the h/l ratio. The value of τ_{late} appears to be basically unaffected by the h/l ratio; how-

ever, significant changes in τ_{early} occur when the h/l ratio is equal to or less than one. For an h/l ratio change of 50 to 0.5; the value of the maximum S/N decreases by approximately a factor of 2.

Effect of pulse length. The effect of a finite length current pulse can be studied if we assume that the secondary field caused by the current turn-on is equal, but opposite, that of the current turn-off. We further assume that the target response has an exponential decay ($e^{-\tau/\zeta}$) and that the overburden response decays according to a power law ($\tau^{-\nu}$). Thus, the observed S/N will be modified when using a finite current pulse as follows:

$$\text{S/N}_{\text{modified}} = \frac{1 - e^{-\Delta/\zeta}}{1 - \left[1 + \frac{\Delta}{\tau}\right]^{-\nu}} \text{S/N}_{\text{original}}, \quad (5)$$

where the pulse length equals Δ. For targets beneath conductive overburden, equation (5) can be expected to hold after the target response peaks. The modification predicted by equation (5) will, in most cases, lead to a reduction in the S/N.

Voltage measurements. Most EM field systems measure the voltage induced in a receiver coil rather than the detected magnetic field. Because the observed voltage response is proportional to the time derivative of the magnetic field, the response of a target beneath overburden will show a change in sign as the secondary field first grows and then decays. If we again assume an exponential decay for the target response and a power law decay for the overburden, then the late-time change in the S/N for a voltage detector is:

$$\text{S/N}_{\text{modified}} = \left[\frac{\nu\tau}{\zeta}\right] \text{S/N}_{\text{original}}. \quad (6)$$

The early-stage voltage response of a target beneath overburden can certainly not be predicted by reference to a free-space model. After the voltage response changes sign (magnetic field peaks), however, a free-space model can reasonably predict the target response. From equation (6), we see that in some circumstances the voltage response may give a higher S/N than the original magnetic field response.

Conclusions

The case of target detection beneath conductive overburden in time-domain EM has been studied for the horizontal coaxial dipole configuration. The main objective of this study was modeling of the target response with consideration of its location beneath the overburden. The anomalous magnetic field response of the target must first build up, because of the screening effects of the overburden, and then decay. The target response will exceed the overburden response for a certain time window which depends on many factors: target-overburden conductance contrast, target depth, target size, and height-to-dipole separation ratio. An enhancement of the target response, over the free-space prediction, is seen with a finite resistivity host rock, but the host rock resistivity was not found to be critical in determining target detection capability. An EM system with a large h/l ratio was found to have the best target detection capability, which diminished as the h/l ratio lessened. A finite length current pulse will generally not enhance the S/N. Measurement of the voltage response, rather than the magnetic field response, can yield a higher S/N at certain late times.

While the particular system configuration studied is not widely used, the conclusions should be applicable in other situations. The effect of conductive overburden in time-domain EM is to delay the time of detection of a conductive target beneath it. Thus an explorationist can enhance his prospects of finding a buried conductor by changing his survey parameters to ensure signal detection in the appropriate time window.

Acknowledgments

We would like to acknowledge the financial support of Selco Div. of British Petroleum Canada for this study. We would also like to thank Dr. KiHa Lee, of Lawrence Berkeley Laboratory, for his assistance in setting up the SHEET program.

References

Fuller, B. D., 1971. Electromagnetic response of a conductive sphere surrounded by a conductive shell: Geophysics, **36**, 9–24.
Grant, F. S., and West, G. F., 1965, Interpretation theory in applied geophysics: McGraw-Hill Co., Inc.
Kaufman, A. A., 1978, Frequency and transient responses of electromagnetic fields caused by currents in confined conductors: Geophysics, **43**, 1002–1010.
Nabighian, M. N., 1971, Quasi-static transient response of a conducting permeable two-layer sphere in a dipolar field: Geophysics, **36**, 25–37.
Spies, B. R., 1980, TEM in Australian conditions: Field examples and model studies: Ph.D. thesis, Macquarie Univ.
Weidelt, P., 1981, Report on dipole induction by a thin plate in a conductive halfspace with an overburden: Research project NTS 83 (BMFT), Fed. Int. for Earth Sciences and Raw Materials, Hannover, W. Germany, archive no. 89727.

Effects of Vertical Contacts on Time-Domain Electromagnetic Sounding MIN 1.8

M. J. Wilt and A. Becker, University of California, Berkeley

We investigated the anomalous effects of a vertical geologic contact on transient electromagnetic sounding (TEM) measurements. The magnetic field responses for this simple feature were studied using a laboratory scale model assembled at the University of California, Berkeley. Models were made for (1) a discontinuous conductive surface layer (surface contact), and (2) a surface contact with a deeper conductive layer present. These models were studied using five TEM sounding configurations: (1) central loop, (2) fixed-separated loops oriented perpendicular to the contact, (3) fixed-separated loops parallel to the contact, (4) fixed transmitter loop-variable offset receiver, and (5) electrical dipole transmitter-variable offset receiver.

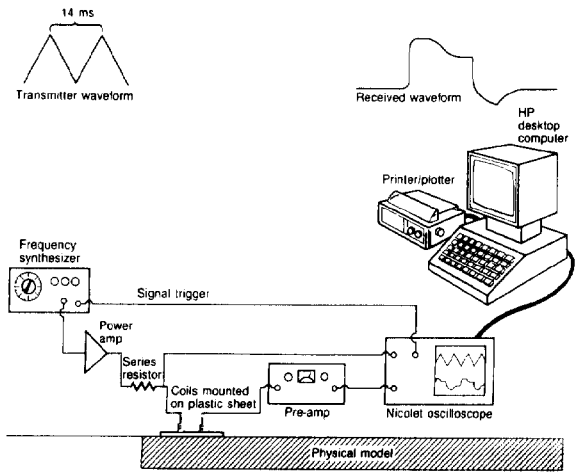

FIG. 1. Scale model system.